

omni

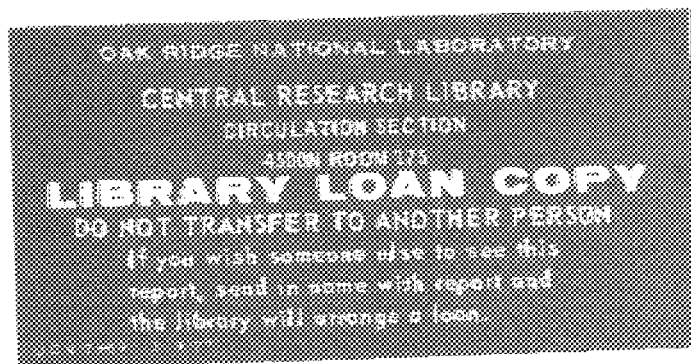
ORNL/TM-8819

OAK
RIDGE
NATIONAL
LABORATORY



Corrosion of Fluidized-Bed Boiler Materials in Synthetic Flue Gas

J. I. Fedarar



OPERATED BY
UNION CARBIDE CORPORATION
FOR THE UNITED STATES
DEPARTMENT OF ENERGY



ORNL/TM-8819
Distribution
Category UC-95

METALS AND CERAMICS DIVISION

CORROSION OF FLUIDIZED-BED BOILER MATERIALS
IN SYNTHETIC FLUE GAS

J. I. Federer

NOTICE: This document contains information of
a preliminary nature. It is subject to revision
or correction and therefore does not represent
a final report.

Date Published: November 1983

Prepared by the
OAK RIDGE NATIONAL LABORATORY
Oak Ridge, Tennessee 37830
operated by
UNION CARBIDE CORPORATION
for the
Office of
Industrial Programs
U.S. Department of Energy
under Contract No. W-7405-eng-26

CONTENTS

ABSTRACT 1
INTRODUCTION 1
DESCRIPTION OF FLUIDIZED-BED WASTE HEAT RECOVERY SYSTEM 3
PREVIOUS CORROSION STUDIES 5
SPECIMEN PREPARATION 9
TEST CONDITIONS 10
RESULTS 13
 CORROSION RATES 13
GENERAL APPEARANCE AND MICROSTRUCTURE 17
DISCUSSION AND CONCLUSIONS 21
ACKNOWLEDGMENTS 26
REFERENCES 27

CORROSION OF FLUIDIZED-BED BOILER MATERIALS IN
SYNTHETIC FLUE GAS*

J. I. Federer

ABSTRACT

Candidate materials for components of a fluidized-bed waste heat recovery system (FBWHRS) include plain carbon steel, types 405 and 316 stainless steel, and alloy 800. These materials were exposed to synthetic flue gas at anticipated FBWHRS temperatures and higher for 3000 h to determine corrosion rates. The synthetic flue gas was a combustion atmosphere to which Cl_2 and HCl were added. The projected annual corrosion rate for plain carbon steel is about 0.08 mm/year (0.003 in./year) at 250 to 290°C, but it would exceed 0.5 mm/year (0.02 in./year) at 560°C. The projected annual corrosion rates of the other materials were less than 0.25 mm/year (0.01 in./year) at the maximum test temperatures of 560, 660, and 665°C for type 405, type 316, and alloy 800, respectively. These results indicate that corrosion of candidate FBWHRS materials will not be significant at anticipated operating temperatures for various components unless other factors, not included in this study, cause accelerated corrosion.

INTRODUCTION

Regenerators and recuperators have been used for many years to recover waste heat from industrial processes. For example, heat recovered from flue gases is used to preheat raw materials or combustion air or to generate steam, thereby decreasing the use of fuel. High temperatures, corrosive species, and particulates that erode or foul heat recovery devices characterize the flue gases from some industrial furnaces, for example, aluminum remelt, steel soaking pit, and glass furnaces. In recent years the opportunity for greater fuel savings through higher preheat air temperatures has been pursued. As a result research and development on more durable ceramic materials and on ceramic recuperator technology have increased. Recuperators having SiC tubes as the heat transfer

*Research sponsored by the Office of Industrial Programs, U.S. Department of Energy under contract W-7405-eng-26 with Union Carbide Corporation.

elements are being developed by private industry under contracts with the U.S. Department of Energy (DOE) and the Gas Research Institute.^{1,2}

Another approach to waste heat recuperation is represented by fluidized-bed heat exchangers, also being developed by private industry under contract to DOE. One of these concepts is a fluidized-bed waste heat recovery system (FBWHRS) that converts waste heat to steam. Flue gases fluidize and heat the bed media, which in turn transfer heat to the steam generator tubes. This type of device has been successfully used to recover heat from flue gases of diesel engines on seagoing vessels. Application to industrial furnaces requires advances in technology because the device will operate at higher temperatures. Although heat is not recovered at high temperatures, as is done by ceramic recuperators, the fluidized-bed boiler has the following attractive features for waste heat recovery:

- proven method,
- high effectiveness,
- design temperatures that allow use of metallic alloys for most components, and
- removal of fouling deposits by periodic cleaning of distributor plate.

Aerojet Energy Conversion Company will design, construct, install, and operate a full-scale FBWHRS as a demonstration of performance and reliability.³ The initial site selected for the unit was an aluminum remelt furnace fired with natural gas. The furnace operates on a 3-h cycle as follows:

- charge melting (high firing), 2.0 h;
- fluxing with Cl_2 gas, 0.25 h; and
- discharge (nonfiring), 0.75 h.

Chlorine fluxing is a common industrial procedure for purifying molten aluminum. Certain impurities, such as magnesium, are converted to chloride compounds that can be separated from the melt. During fluxing and nonfiring portions of the cycle, flue gases would bypass the FBWHRS. The flue gases would pass through the fluidized-bed boiler only during the

high-firing portion of the cycle. Although Cl_2 is not added to the melt during high firing, residual Cl_2 and HCl are present in the flue gases. The corrosive potential of flue gases containing Cl_2 and HCl needed to be assessed because serious corrosion would affect both performance and reliability.

The purpose of this investigation was to develop a data base for corrosion of candidate construction materials. This information was needed for selection of materials for boiler components, namely, distributor plate, steam generator tubes, and containment walls. The task was accomplished by reviewing pertinent corrosion literature and by conducting corrosion tests. In the latter case unstressed candidate materials were exposed to synthetic flue gases containing Cl_2 and HCl at and above anticipated FBWHRs use temperatures for 3000 h. Annual corrosion rates were projected from the results of the test.

DESCRIPTION OF FLUIDIZED-BED WASTE HEAT RECOVERY SYSTEM

The fluidized-bed boiler is shown schematically in Fig. 1. Flue gases, diluted with air to lower their temperature to about 600°C , are

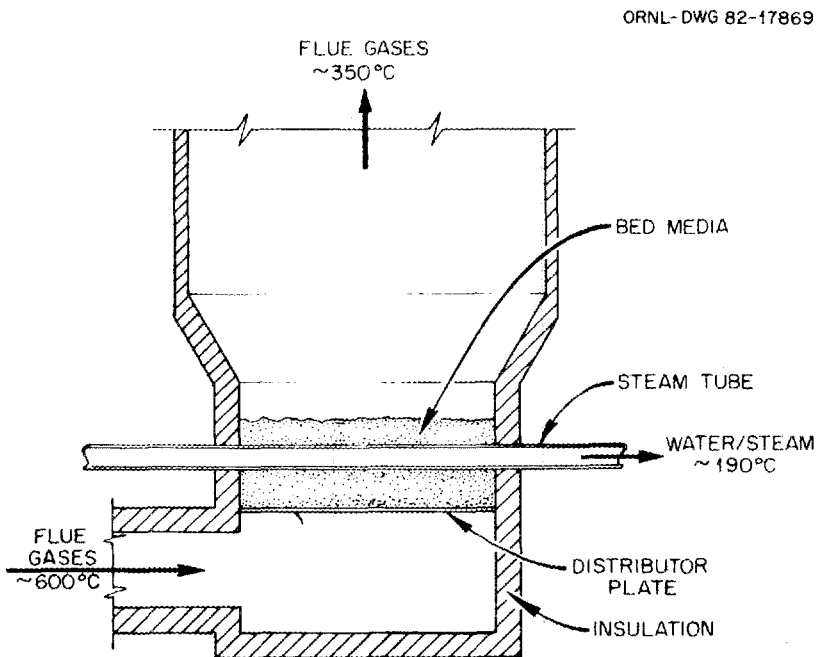


Fig. 1. Fluidized-bed waste heat recovery system boiler.

diverted from the main flue into the boiler. The gases enter the boiler through openings in the distributor plate, which forms the base of the bed. (In an advanced version the inlet gas temperature may be as high as 1000°C.) The gases fluidize and heat the aluminum oxide bed medium, which is kept shallow to minimize the pressure drop through the boiler. Heat is transferred from the bed to the steam tubes, with the surface temperature of the tubes and containment wall maintained at 250 to 290°C. The exit gas temperature is about 350°C. All components in the bed are subjected to the eroding action of the bed medium.

Candidate reference and alternative materials for distributor plate, steam tubes, and containment wall are metals. Their compositions and maximum anticipated use temperatures in the boiler are shown in Table 1. In each case the alternative is more oxidation resistant than the reference material. Type 347 stainless steel, a stabilized grade, which resists precipitation of carbides at grain boundaries, was included for comparison. Tentative selection of these materials reflects the intent to construct the boiler with common structural materials, for which fabrication technology, availability, and cost are well established.

Table 1. Candidate materials for fluidized-bed waste heat recovery system boiler components

Component	Material	Nominal composition (wt%)				Estimated temperature in FBWHRs (°C)
		Cr	Ni	Fe	Other ^a	
<i>Distributor plate</i>						
Reference	Type 316 SS	17	12	Bal	2 Mo	600
Alternative	Alloy 800	21	33	Bal		600
(For comparison)	Type 347 SS	18	11	Bal	Nb + Ta ^b	
<i>Steam tubes and containment walls</i>						
Reference	Plain carbon steel			~99		250-290
Alternative	Type 405 SS	13		Bal	0.2 Al	250-290

^aThese materials also contain small amounts of C, Mn, Si, P, and S.

^bConcentration is 10 times carbon content.

PREVIOUS CORROSION STUDIES

Related corrosion studies have involved exposure of materials to essentially pure Cl_2 or HCl gases and to actual and simulated combustion atmospheres containing these gases. Although exposure to pure Cl_2 or HCl would be an unlikely event for the fluidized-bed heat exchanger, the results of these tests were reviewed for possible assistance in interpreting corrosion behavior in combustion atmospheres. Results from previous studies are summarized in Table 2.

Heinemann, Garrison, and Haber exposed steel to dry Cl_2 gas at 77 to 251°C for up to 8 h (ref. 4), and Brown, DeLong, and Auld exposed a variety of materials including steel and type 316 stainless steel in dry Cl_2 , in dry HCl , and in these gases with additions of H_2O , air, or SO_2 (ref. 5). Temperatures of interest to the fluidized-bed heat exchanger were included in these studies, but test periods were only 20 h or less. A maximum corrosion rate of 3.5 $\mu\text{m}/\text{h}$ was obtained by Brown and coworkers at the temperatures shown in Table 2 for steel and type 316 stainless steel.⁵ Although this corrosion rate projects to an annual rate of about 31 mm/year, such a projection is not justified because corrosion rates usually decrease with increasing exposure time unless corrosion products are somehow removed. In both studies corrosion rates were roughly proportional to the vapor pressure of the principal reaction product, which in the case of iron-base alloys was ferric chloride. The study by Brown and coworkers revealed higher corrosion rates in dry Cl_2 than in dry HCl (ref. 5). Higher corrosion rates were obtained when Cl_2 -0.4% H_2O and HCl -0.2% H_2O were used until a temperature of 371°C was reached. Above 371°C corrosion rates were the same as those obtained with dry Cl_2 and HCl . Corrosion rates in HCl -air and HCl -10% SO_2 mixtures were similar to those obtained with dry HCl .

Miller and Krause reported a maximum corrosion rate of about 1.5 $\mu\text{m}/\text{h}$ for steel, low-alloy steel, and types 304 and 321 stainless steel exposed for 122 to 389 h to combustion gases containing SO_2 and HCl (ref. 6). Electron microprobe analysis revealed the presence of Cl, S, Pb, Zn, Fe, Na, K, Ca, Al, Si, Sn, Ni, and Cr in the corrosion product or at the

Table 2. Summary of corrosion results obtained by other investigators

Material	Atmosphere	Test period (h)	Temperature (°C)	Corrosion rate (µm/h)	Source, reference
Steel	Dry Cl ₂	8 Max	77-251	0.02-0.03	Heinemann, Garrison, Haber ⁴
Steel	Dry Cl ₂	20 Max	121-232	0.1-3.5	Brown, DeLong, Auld ⁵
Type 316	Dry Cl ₂	20 Max	316-482	0.1-3.5	
Steel	Dry HCl	20 Max	260-621	0.1-3.5	
Type 316	Dry HCl	20 Max	371-649	0.1-3.5	
Steel, 1.25 Cr-0.5 Mo	Combustion gases with 90-115 ppm HCl and 40-106 ppm SO ₂	122-389	177-427	0.5-1.4	Miller, Krause ⁶
			191-413	0.6-1.7	
Type 304			413-607	0.5-1	
Type 321			454-621	1-1.5	
Steel	Synthetic combustion gases with 250 ppm SO ₂	Not given	427-538	0.02-0.2	
Steel	Synthetic combustion gases with 250 ppm SO ₂ and 200 ppm HCl	Not given	427	0.03	
Steel	Combustion gases with 2-303 ppm SO ₂ and 5-115 ppm HCl	828	204-454	0.1-0.5	Krause, Vaughn, Miller ⁷
Steel, 1.25 Cr- 0.5 Mo	Combustion gases with ~3-300 ppm HCl, SO ₂ not given	Not given	163-510	0.5-1.8	Krause, Vaughn, Miller ⁸
Types 304 and 321, Incoloy 825			329-649	0.4-1.4	

Table 2. (continued)

Material	Atmosphere	Test period (h)	Temperature (°C)	Corrosion rate (µm/h)	Source, reference
Steel	Combustion gases with				
	0.5% Cl, 0.25% S	<10	149-593	1.3-5.8	Vaughn, Krause, Boyd ⁹
	0.75% Cl, 0.25% S	<10	149-593	2.8-7.9	
	2.5% Cl, 0.25% S	<10	149-593	2.5-14.0	
	0.5% Cl, 1.0% S	<10	149-593	1.3-8.1	
0.5% Cl, 1.75% S	<10	149-593	0.3-3.1		
Type 316	0.5% Cl, 0.25% S	<10	593	1.5	
	0.75% Cl, 0.25% S	<10	593	3.1	
	2.5% Cl, 0.25% S	<10	593	1.8	
	0.5% Cl, 1.0% S	<10	371-593	0.1-0.3	
	0.5% Cl, 1.75% S	<10	371-593	0.1-0.4	
Incoloy 825	0.75% Cl	<10	371	2.5	
	2.5% Cl	<10	371	0.5	
Steel	Synthetic combustion gases:	~256	540	0.1	Mayer, Manolescu ¹⁰
	14.1% CO ₂ , 81.5% N ₂ , 4.0% O ₂ ,		700	0.2	
	0.2% CO, 0.2% SO ₂ ,		1000	13	
	0.1% HCl				
1.25 Cr-0.5 Mo		~256	540	0.1	
			700	0.2	
			1000	14	
Type 321		~450	540	0.01	
			700	0.05	
			1000	3.3	

corrosion interface in most specimens. The exposure period also included intervals during which the specimens were at temperatures below 200°C in moisture-containing atmospheres. Corrosion rates lower than 1.5 $\mu\text{m}/\text{h}$ were obtained for steel (at comparable temperatures) exposed to synthetic combustion atmospheres containing either SO_2 or SO_2 plus HCl .

Krause, Vaughn, and Miller⁷ obtained a maximum corrosion rate of about 0.5 $\mu\text{m}/\text{h}$ for steel exposed 828 h to a combustion atmosphere similar to that used by Miller and Krause.⁶ The lower corrosion rate that they obtained might reflect the frequent observation that initially high corrosion rates gradually decrease with increasing exposure time.

Krause, Vaughn, and Miller reported maximum corrosion rates of 1.8 $\mu\text{m}/\text{h}$ for steel and a low-alloy steel and 1.4 $\mu\text{m}/\text{h}$ for types 304 and 321 stainless steel and Incoloy 825 at the temperatures shown in Table 2 (ref. 8.) The corroding environment was a combustion atmosphere containing HCl and possibly SO_2 . The corrosion rates were similar to those reported by Miller and Krause;⁶ in fact, these might be substantially the same data.

In tests of 10 h or less Vaughn, Krause, and Boyd determined corrosion rates of steel, type 316 stainless steel, and Incoloy 825 exposed to combustion gases containing additions of sulfur as the element and chlorine as polyvinyl chloride.⁹ The data indicate that the corrosion rate of steel increased with increasing chlorine content at constant sulfur content. At constant chlorine content the corrosion rate passed through a maximum with increasing sulfur content. The corrosion rate of type 316 stainless steel decreased with increasing sulfur content, and the corrosion rate of Incoloy 825 decreased with increasing chlorine content. These trends, however, are based on short exposure times and might not continue with longer exposure. Other data, not shown in Table 2, indicated that corrosion rates increased with increasing combustion gas temperatures, suggesting that specimen surface temperatures were actually higher than were recorded.

Mayer and Manolescu studied corrosion of materials in synthetic combustion gases containing SO_2 and HCl at 540, 700, and 1000°C (ref. 10). Corrosion rates in the synthetic combustion gases were lower (at comparable

or even higher temperatures) than reported by Miller and Krause⁶ for the same materials exposed to actual combustion gases containing approximately the same amounts of SO₂ and HCl. The difference might have been caused by one or more metallic elements in the actual combustion atmospheres used by Miller and Krause, who also obtained lower corrosion rates in synthetic atmospheres.⁶

In summary, previous studies of corrosion of steels, stainless steels, and a nickel-base alloy have been conducted in Cl₂ and HCl gases and in actual and simulated combustion atmospheres. Test periods ranged between a few hours and about 800 h. Corrosion rates were higher in actual combustion atmospheres than in simulated atmospheres. The corrosion rate of steel increased with increasing HCl content in the combustion atmosphere. Stainless steels, as expected, were more resistant to corrosion than was steel or low-alloy steels. Corrosion rates were 0.1 μm/h or more during typical test periods of a few hundred hours. Although 0.1 μm/h projects to an annual corrosion rate of 0.87 mm/year (0.034 in./year), such a projection is not justified because actual corrosion rates usually decrease with time unless corrosion products are nonpassivating or their removal is accelerated.

SPECIMEN PREPARATION

Specimens measuring approximately 25 by 38 by 3 mm were cut from sheet stock of plain carbon steel, types 316 and 347 stainless steel, and alloy 800. Specimens of type 405 stainless steel were obtained from 13-mm-OD by 0.9-mm-thick-wall tubing by first cutting 38-mm-long sections, then cutting each section along a diametral plane. Holes measuring about 2 mm in diameter near one end allowed the specimens to be hung from a rack during the exposure.

Specimens were tested in as-received, annealed, and welded conditions. The microstructures and corrosion behavior of as-received materials, as will be shown, were substantially the same as those of materials that had been annealed. The annealing conditions were as follows:

- plain carbon steel and type 405 stainless steel — 910°C, 10 min, helium atmosphere, furnace cooled;
- types 316 and 347 stainless steel — 1075°C, 15 min, helium atmosphere, water quenched; and
- alloy 800 — 1050°C, 5 min, helium atmosphere, cooled by transferring specimens to water-cooled zone of furnace tube.

Welded specimens were prepared by forming a fusion zone along the longitudinal centerline of specimens in the as-received condition. The gas tungsten arc process was used without addition of filler metal. All specimens were grit blasted, rinsed in alcohol, and dried before installation in the test furnace.

TEST CONDITIONS

Specimens hung from a rack in a 62-mm-ID ceramic tube (long axis horizontal) heated by a furnace. Because a temperature gradient occurred along the furnace, the location determined specimen temperatures. The specimens hung three abreast as shown schematically in Fig. 2 and in the photograph in Fig. 3. The type 405 stainless steel and plain carbon steel specimens were located at the gas inlet and outlet ends of the heated zone, respectively, and the other specimens were located at intermediate hotter positions. Specimens hung with long dimensions vertical, spaced about 25 mm apart in the longitudinal direction of the furnace tube and 10 mm apart in the diametral direction.

Synthetic flue gases were prepared by mixing air, N_2 , CO_2 , H_2O , Cl_2 , and HCl . Each gas except H_2O was metered with conventional tube-and-float flowmeters. The N_2 and CO_2 bubbled through water at about 44°C, resulting in transfer of about 5 g/h of water vapor into the furnace tube. The total flow rate of gases required less than 1 cm^3/min each of Cl_2 and HCl to obtain the desired concentrations. Because such low flow rates could not be metered with existing flowmeters, a mixture of air, Cl_2 , and HCl was prepared by metering 4700 cm^3/min of air and 10 cm^3/min each of Cl_2 and HCl into a manifold. Most of this mixture was vented; however,

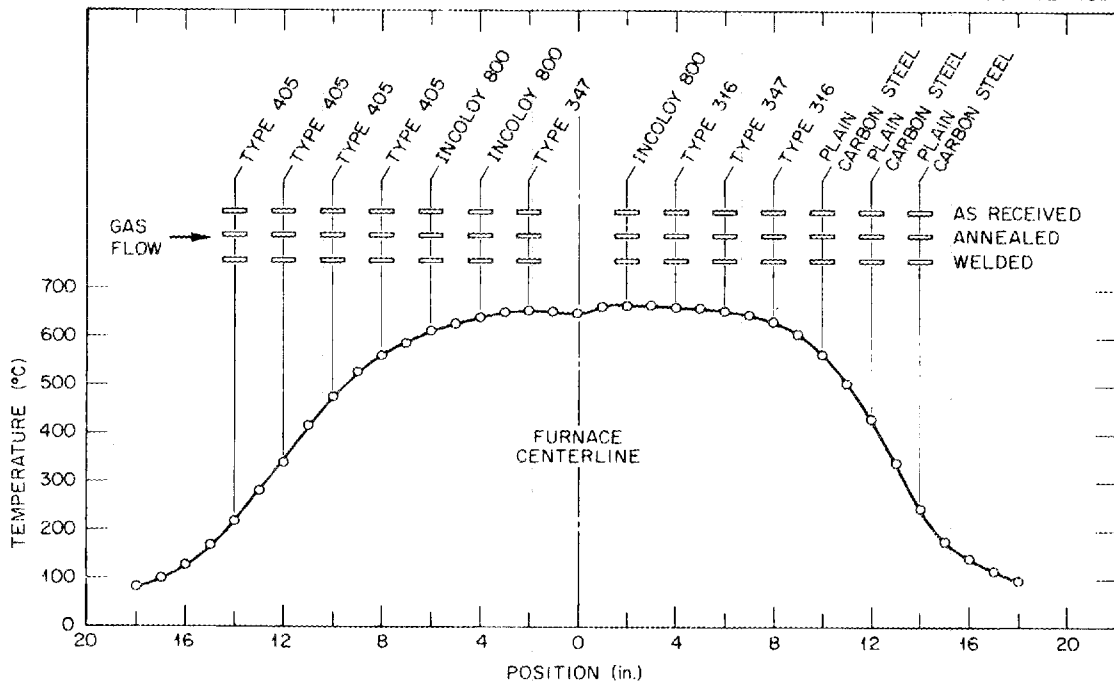


Fig. 2. Schematic representation of specimens in furnace during exposure to synthetic flue gas; 1 in. = 25.4 mm.

Y-185198

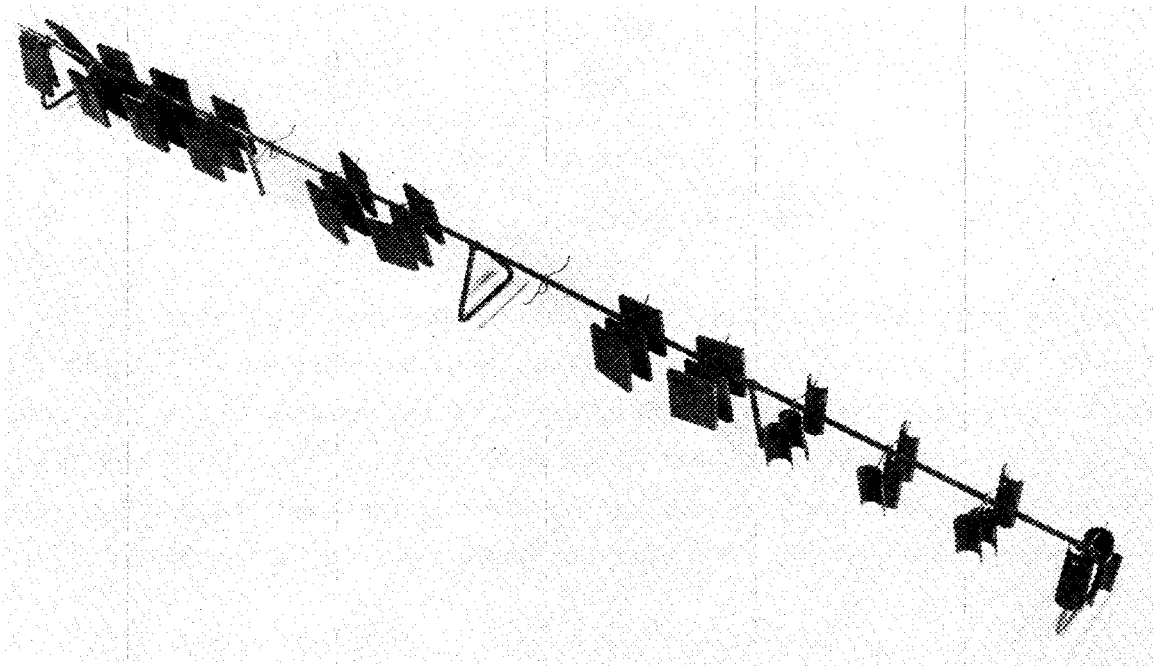


Fig. 3. Specimens on rack for exposure test. Flat specimens are 25 by 38 by 3 mm.

200 cm³/min of the mixture containing about 0.2 vol % each of Cl₂ and HCl was metered into the furnace tube along with the other gases. The indicated flow rates of individual gases in the mixture are shown in Table 3. The total chloride content in the mixture was determined by bubbling the mixture through two successive 0.1 N NaOH solutions to capture HCl and Cl₂. Analysis of the solutions indicated that the gas mixture contained 0.024 vol % total chloride at the inlet end of the furnace compared with 0.014 vol % total chloride indicated by the flowmeters. After contacting the specimens at temperature, the mixture contained by analysis 0.019 vol % total chloride. The analyses therefore indicated that the HCl and Cl₂ flow rates were higher than intended. The total volumetric gas flow rate was 5960 cm³/min, and the linear flow rate was 200 cm/min.

Table 3. Composition of synthetic flue gases

Gas	Flow rate ^a (cm ³ /min)	Concentration (vol %)
N ₂	4700	79
O ₂	1020	17
CO ₂	120	2
H ₂ O	120	2
Cl ₂	0.4	0.012
HCl	0.4	0.012

^aMeasured at about 25°C except H₂O, which was not directly metered.

The candidate materials, their anticipated use temperature in the boiler, and the range of temperatures in this test are shown in Table 4. The test temperature range slightly exceeded the estimated use temperature of type 316 stainless steel and alloy 800. Plain carbon steel and type 405 stainless steel were tested over a wider range, and the maximum test temperature exceeded the estimated use temperature by about 300°C.

Table 4. Conditions of corrosion test

Atmosphere:	Synthetic flue gas	
Duration:	3000 h with intermediate measurements after 500 and 1500 h	
Temperature, °C		
Plain carbon steel	240-560 (250-290) ^a	
Type 405	220-560 (250-290) ^a	
Type 316	625-660 (600) ^a	
Alloy 800	605-665 (600) ^a	
Type 347	650 (600) ^a	

^aAnticipated temperature in fluidized-bed waste heat recovery system.

RESULTS

CORROSION RATES

The thickness of uncorroded specimens of each material in as-received and annealed conditions was measured on polished samples on an optical metallograph with an integral calibrated scale. At least three measurements were made at different locations to obtain an average pretest thickness X_0 . Similarly the average thickness of unattacked metal X_1 was measured on corroded samples. The thickness of unattacked metal was measured from the deepest grain boundary penetration on one side of the sample to the deepest penetration on the other side. The depth of corrosion d was then calculated from the expression $d = (X_0 - X_1)/2$.

The corrosion results are summarized in Table 5. The depth of corrosion of plain carbon steel in both the as-received and annealed conditions increased with both time and temperature, and the corrosion rate increased with temperature. The annual corrosion rate projected linearly from the results after 3000 h ranged from about 0.04 mm/year (0.002 in./year) at 240°C to 0.59 mm/year (0.023 in./year) at 560°C. At the estimated use temperature for this material (250-290°C) the projected annual corrosion rate is about 0.1 mm/year (0.004 in./year). The depth of corrosion and corrosion rate of type 405 stainless steel were substantially the same in both conditions. The linearly projected annual corrosion rate at 560°C is only about 0.08 mm/year (0.003 in./year) compared with about 0.59 mm/year (0.023 in./year) for plain carbon steel.

Table 5. Summary of corrosion results for candidate materials exposed to synthetic flue gases

Material	Condition	Temperature (°C)	Depth of corrosion (μm) for cumulative exposure times (h) of			Corrosion rate (nm/h) for cumulative exposure times (h) of			Corrosion rate projected from 3000-h exposure	
			500	1500	3000	500	1500	3000	(mm/year)	(in./year)
Plain carbon steel	As received	240	0	10	30	0	7	10	0.09	0.003
		430	3	36	61	6	24	20	0.18	0.007
		560	38	56	155	76	37	52	0.46	0.018
Plain carbon steel	Annealed	240	0	10	15	0	7	5	0.04	0.002
		430	5	18	46	10	12	15	0.13	0.005
		560	41	107	201	82	71	67	0.59	0.023
Type 405 SS	As received	220	0	0	10	0	0	3	0.03	0.001
		340	0	0	13	0	0	4	0.04	0.001
		475	0	0	8	0	0	3	0.03	0.001
		560	5	8	28	10	5	9	0.08	0.003
Type 405 SS	Annealed	220	0	0	23	0	0	8	0.07	0.003
		340	0	0	20	0	0	7	0.06	0.002
		475	0	0	18	0	0	6	0.05	0.002
		560	0	13	20	0	9	7	0.06	0.002
Type 316 SS	As received	625	48	51	64	96	34	21	0.18	0.007
		660	43	53	66	86	35	22	0.19	0.008
Type 316 SS	Annealed	625	48	51	74	96	34	25	0.22	0.009
		660	33	36	56	66	24	19	0.17	0.007
Type 347 SS	As received	650		46			31		0.27	0.011 ^a
Type 347 SS	Annealed	650		46			31		0.27	0.011 ^a
Alloy 800	As received	605	10	20	46	20	13	15	0.13	0.005
		640	15	25	46	30	17	15	0.13	0.005
		665	10	36	38	20	24	13	0.11	0.004
Alloy 800	Annealed	605	15	23	33	30	15	11	0.10	0.004
		640	18	18	28	36	12	9	0.08	0.003
		665	20	25	30	40	17	10	0.09	0.003

^aProjected from 1500-h exposure.

Both type 316 stainless steel and alloy 800 exhibited decreasing corrosion rates with increasing exposure time. Linearly projected annual corrosion rates at 625°C are about 0.20 and 0.10 mm/year (0.008 and 0.004 in./year) for type 316 and alloy 800, respectively. Type 347 stainless steel was tested only during the final 1500-h period. The projected annual corrosion rate based on a 1500-h exposure was about 0.27 mm/year (0.011 in./year). As in the case of previously discussed corrosion results, the linearly projected rates represent maximum values, which would probably not be maintained during longer exposures.

Oxidation of metals often follows the parabolic relationship $X^2 = kt$, where X is the thickness (depth) of oxidized metal, t is time, and k is the parabolic constant. According to this relationship the rate of oxidation, instead of remaining constant, actually decreases with increasing time. Because the relationship derives from an expression for unidirectional diffusion, oxidation by diffusion of metal or oxygen through an oxide layer is the implied mechanism. An essential condition, therefore, for conformance to the parabolic relationship is formation of an adherent oxide layer, the diffusion path. If the oxide layer is periodically disrupted and the metal surface exposed, then the oxidation rate will increase.

If a plot of X vs \sqrt{t} yields a straight line, the data obey the parabolic relationship. The plots for plain carbon steel in Fig. 4 were almost linear at 240 and 430°C, indicating approximate agreement with the parabolic relationship. Plots for plain carbon steel and type 405 stainless steel at 560°C deviated upward, indicating slightly accelerated corrosion rates. The corrosion products that formed at 560°C were shown by x-ray diffraction to be Fe_2O_3 and Fe_3O_4 on plain carbon steel and Fe_2O_3 and FeCr_2O_4 on type 405 stainless steel. These oxides, being less dense than the metals, might have been neither adherent nor protective, as indicated in microstructures to be shown. In addition, loosening or removal of corrosion products during planned interruptions at 500 and 1500 h might have caused higher corrosion rates than would have occurred during an uninterrupted isothermal exposure.

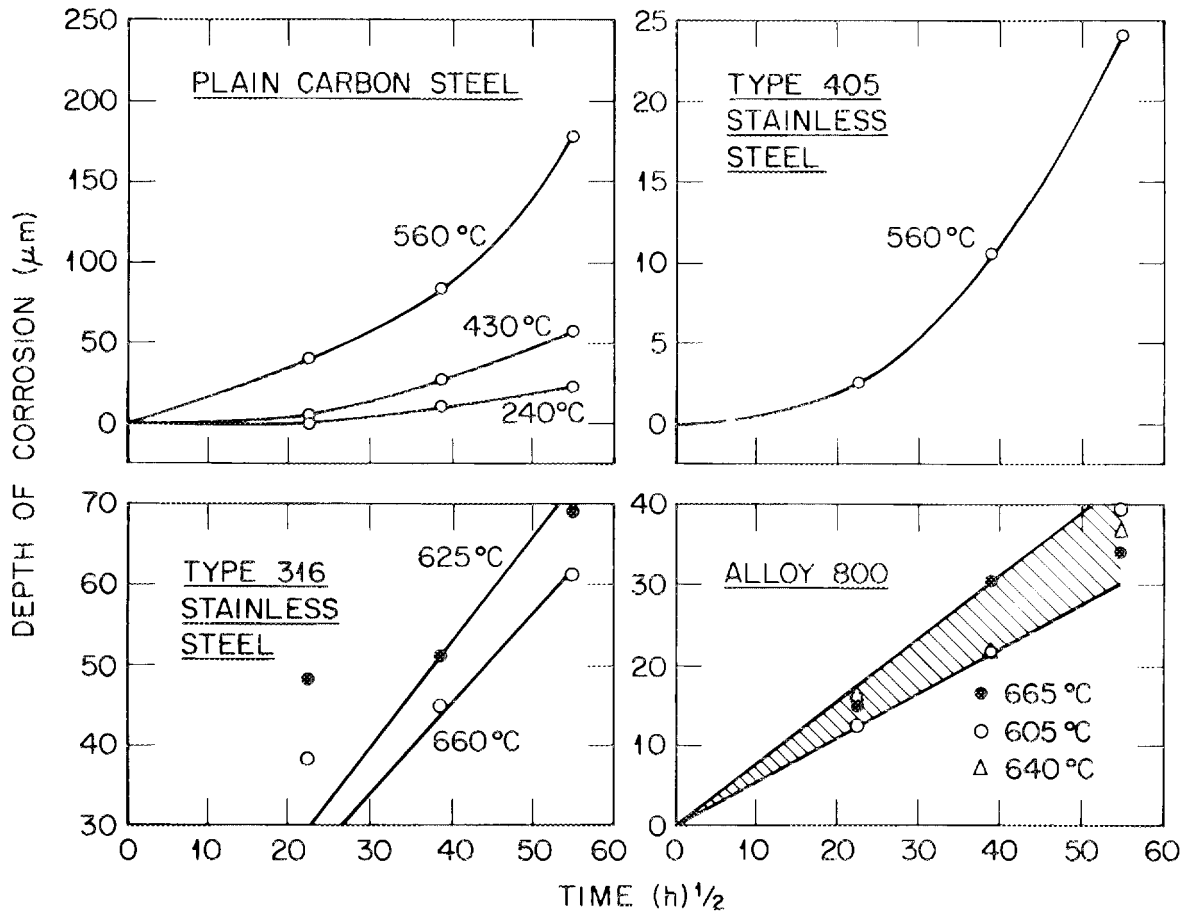


Fig. 4. Depth of corrosion versus $(\text{time})^{1/2}$.

Plots of the data for type 316 stainless steel are linear if the data for 500 h are neglected as shown in Fig. 4. The depths of corrosion at 500 h appear to be unusually large compared with the data at 1500 and 3000 h. Also, the depths of corrosion were higher at 625 than at 660°C, suggesting that measuring errors occurred. The data for alloy 800 can be plotted linearly within the scatter band shown in Fig. 4. These materials would be expected to exhibit linear oxidation behavior (with square root of time) in air at the temperatures of this test because both form adherent protective oxides. The data do not indicate that accelerated corrosion occurred in the simulated flue gas in this test, and corrosion rates actually decreased with time, as shown in Table 5.

GENERAL APPEARANCE AND MICROSTRUCTURE

Plain carbon steel specimens were gray-brown, or brown after exposure. The oxide adhered to specimens exposed at 240°C, became partially detached from specimens exposed at 430°C, and was a loose scale on specimens exposed at 560°C. The oxide on type 405 stainless steel specimens varied from dark brown to reddish brown with increasing exposure temperature and was a loose scale on specimens exposed at 560°C. Type 316 specimens had a mottled gray flaky scale, and alloy 800 had a reddish brown adherent scale.

Typical microstructures of plain carbon steel are shown in Fig. 5. Exposure at 240 and 430°C produced a rough interface between corrosion product and metal, probably because of different rates of attack on grains of different orientation. The interface was smoother at 560°C, and corrosion was significantly faster (Table 5). X-ray diffraction revealed that the corrosion product was hematite (Fe_2O_3) at 240°C and a mixture of hematite and magnetite (Fe_3O_4) at 430 and 560°C. Magnetite, with an oxygen-to-iron ratio of 1.33, is the darker material adjacent to the metal. Electron microprobe analysis did not reveal chlorine in the corrosion product or underlying metal. The limit of detection for chlorine was about 0.1 wt %; therefore, lesser amounts of chlorine might have been present. Microstructures of type 405 stainless steel specimens in Fig. 6 show a rough interface between corrosion product and metal at all test temperatures. Although x-ray diffraction indicated only hematite, the corrosion product of the specimen exposed at 560°C consists of two distinct layers as observed for plain carbon steel at 560°C. Etching the specimen exposed at 560°C showed grain boundary attack near the surface, but electron microprobe analysis did not reveal chlorine in the grain boundaries or in the corrosion product. Chlorine was found in the corrosion product of the specimen exposed at 220°C.

Typical microstructures of type 316 stainless steel specimens are shown in Fig. 7. The grain structure is more clearly outlined in exposed and etched specimens than in the annealed specimen because exposure at 625

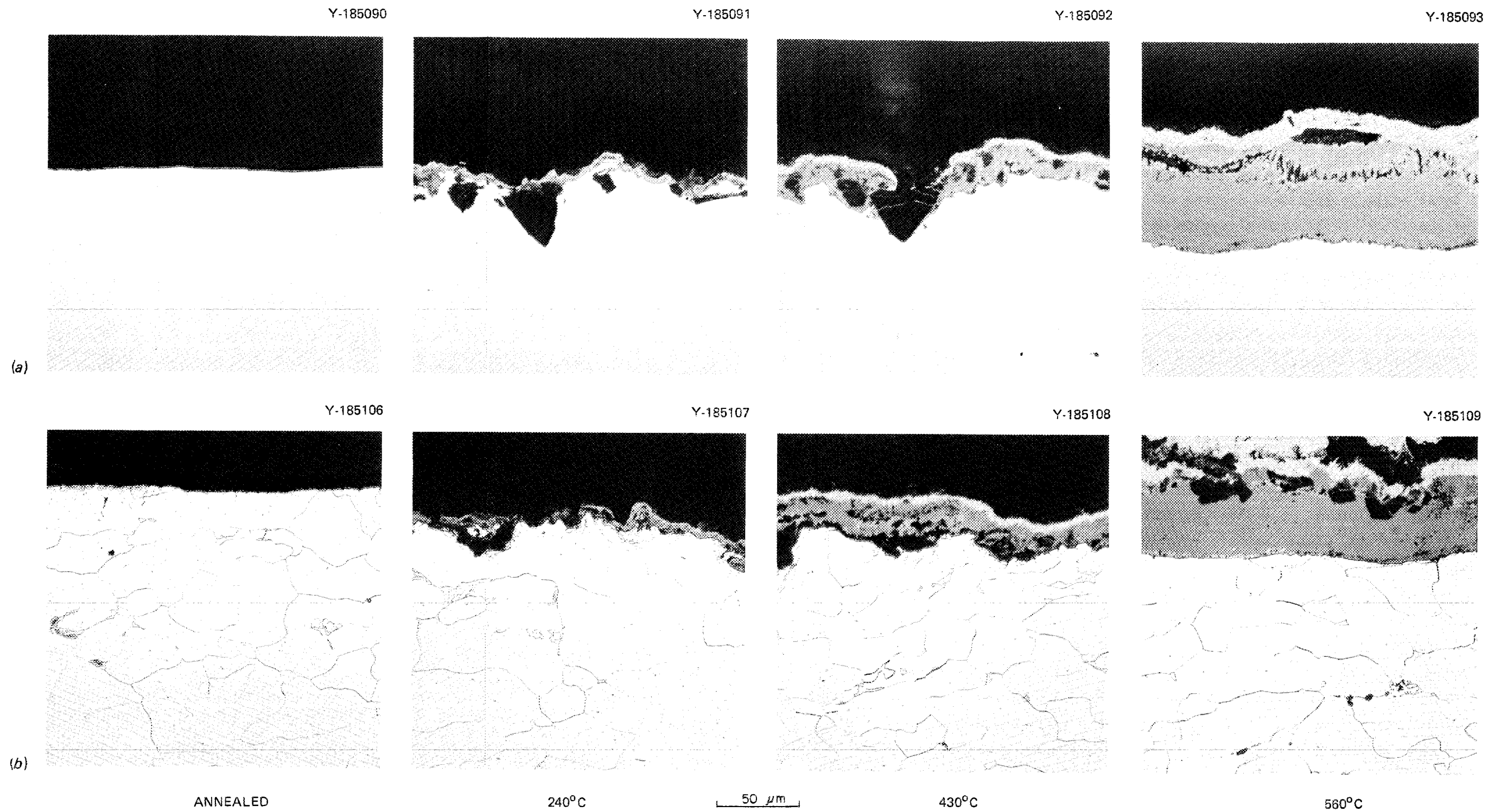


Fig. 5. Microstructures of plain carbon steel. (a) As polished. (b) Etched with 2% Nital. Initial condition and exposure temperatures (500 h) are indicated.

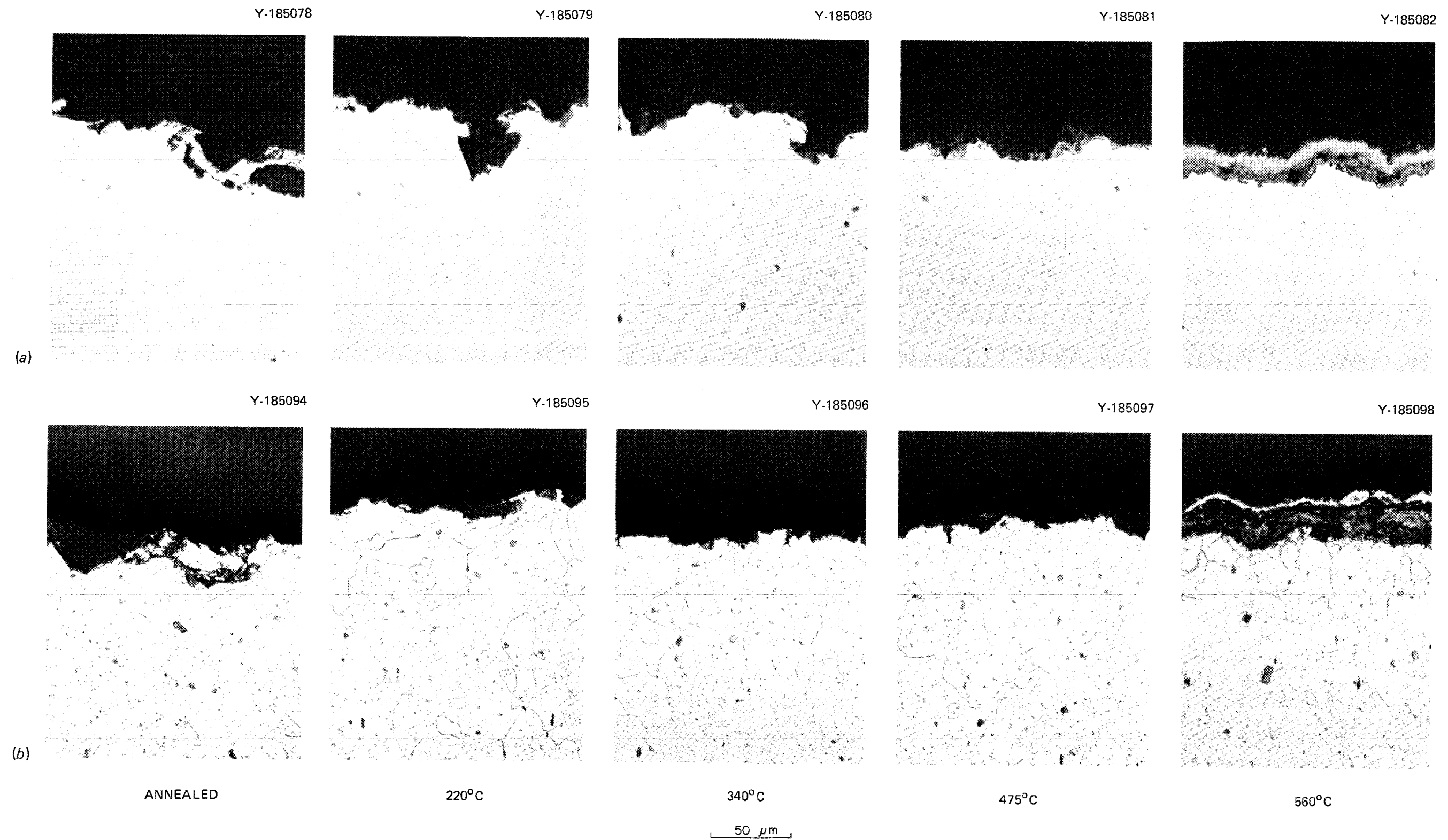


Fig. 6. Microstructures of type 405 stainless steel. (a) As polished. (b) Etched with aqua regia. Initial condition and exposure temperatures (500 h) are indicated.

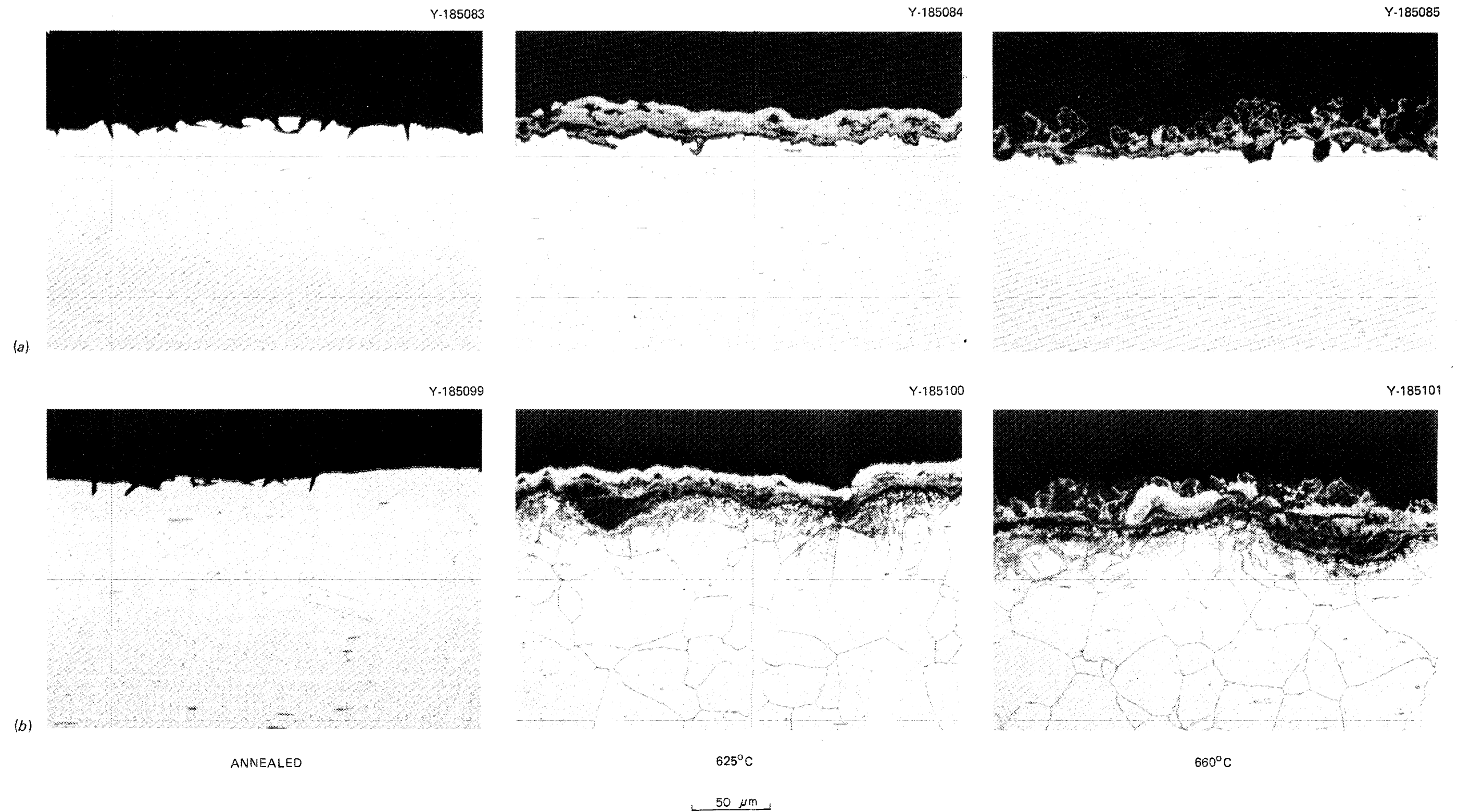


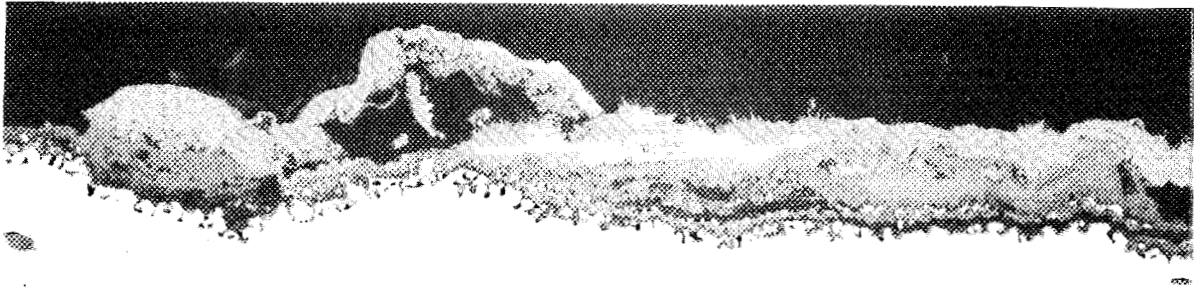
Fig. 7. Microstructures of type 316 stainless steel. (a) As polished. (b) Etched with aqua regia. Initial condition and exposure temperatures (500 h) are indicated.

and 660°C caused precipitation of carbides at grain boundaries. This precipitation causes increased susceptibility to intergranular attack in aqueous solutions. The small amount of corrosion in type 316, however, suggests that grain boundary precipitation did not accelerate corrosion in the gaseous environment of this test. Microstructures of type 347, the stabilized stainless steel, are shown in Fig. 8. The corrosion penetrations in the as-polished sample [Fig. 8(a)] suggest intergranular attack; however, etching revealed that the actual grain size [Fig. 8(b)] was larger than indicated by the corrosive attack. Comparison with type 316 in Fig. 7 shows that grain boundaries were less clearly revealed by etching. Less grain boundary precipitation occurred in type 347 after 1500 h at 650°C than in type 316 after 500 h at 625 and 660°C. The corrosion rates for types 347 and 316 after 1500 h were substantially the same, as shown previously in Table 5. Alloy 800 specimens (Fig. 9) exhibit grain boundary precipitation similar to that in type 316, and grain boundary attack is evident. Nevertheless, corrosion rates for this more oxidation-resistant material were no higher than those for type 316 stainless steel. The corrosion products on type 316 and alloy 800 were hematite, chromia (Cr_2O_3), and chromite (FeCr_2O_4). Electron microprobe analysis did not reveal chlorine in specimens of either material. Figures 7 and 9 show that the corrosion products on both type 316 stainless steel and alloy 800 were partially detached, although this might have occurred during cooling to room temperature.

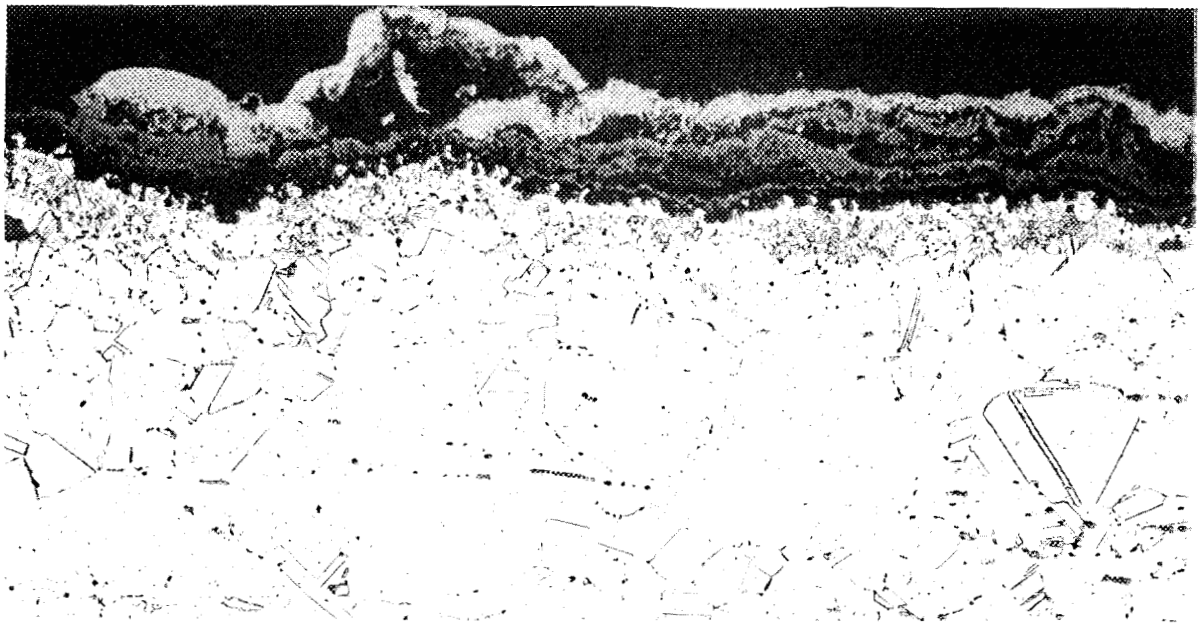
Welded specimens were included in this test to determine if corrosion in the fusion or heat-affected zones occurred at a different rate from that in base metal. Figure 10 shows that corrosion in the weld areas was not substantially different from that in the base material in any of the specimens exposed at the highest temperatures used in this test.

DISCUSSION AND CONCLUSIONS

The results of previous corrosion studies, summarized in Table 2, revealed lower corrosion rates in synthetic flue gases than in actual flue



(a)

50 μm 

(b)

Fig. 8. Microstructures of type 347 stainless steel after 1500 h at 650°C. (a) As polished. (b) Etched.

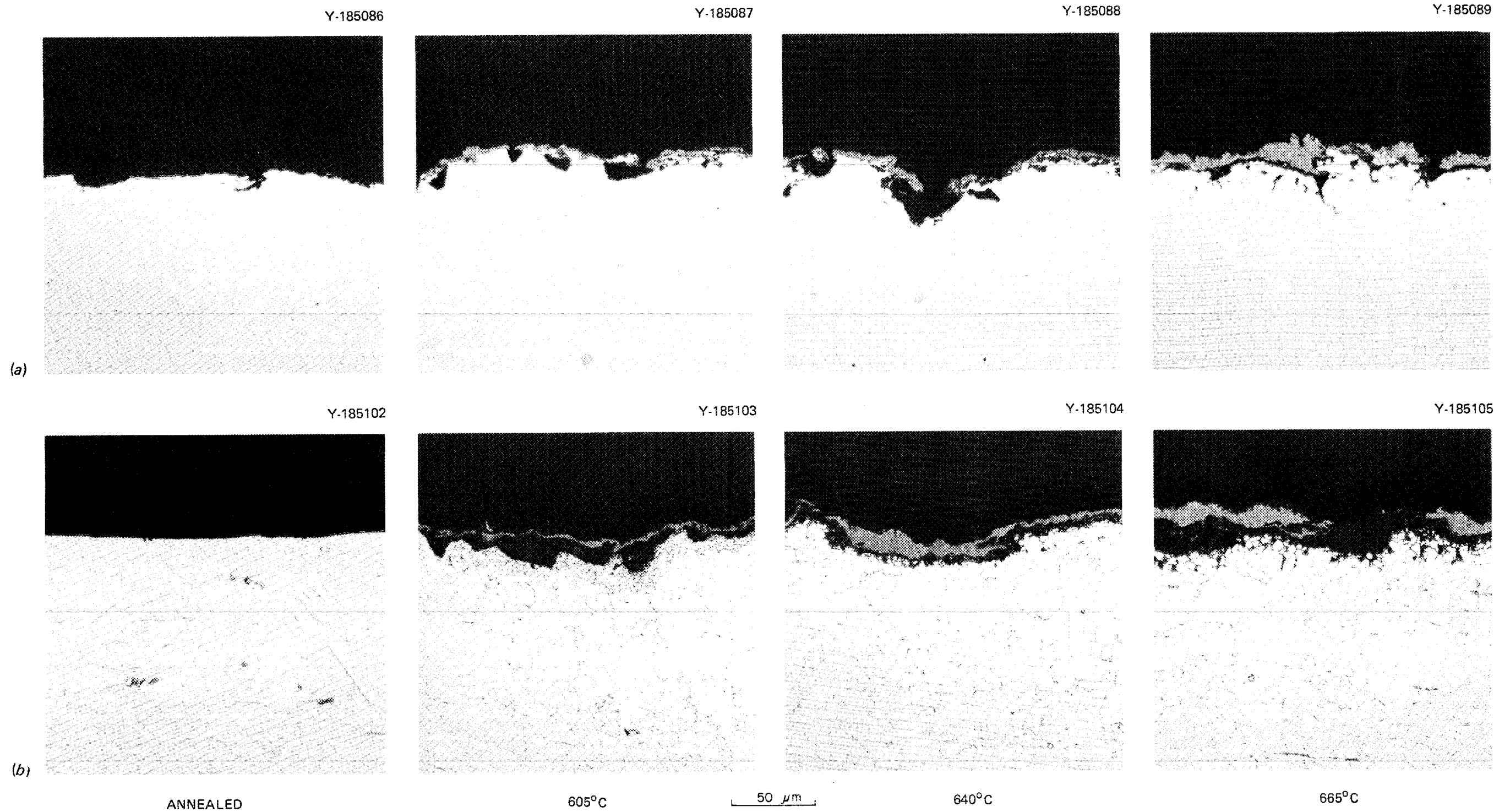
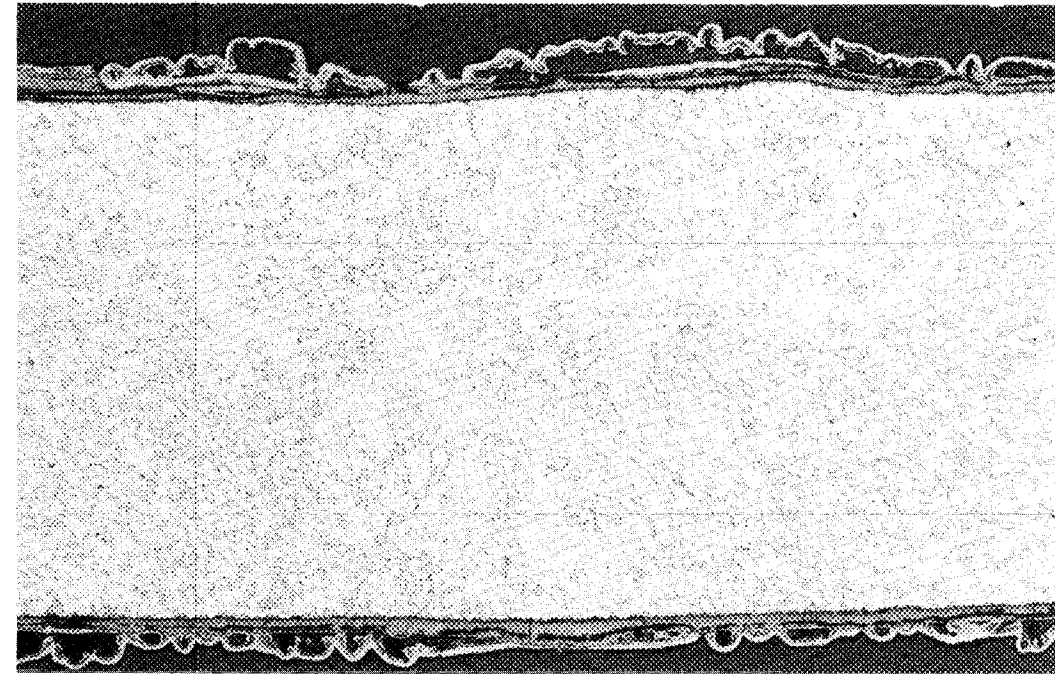


Fig. 9. Microstructures of alloy 800. (a) As polished. (b) Etched with aqua regia. Initial condition and exposure temperatures (500 h) are indicated.

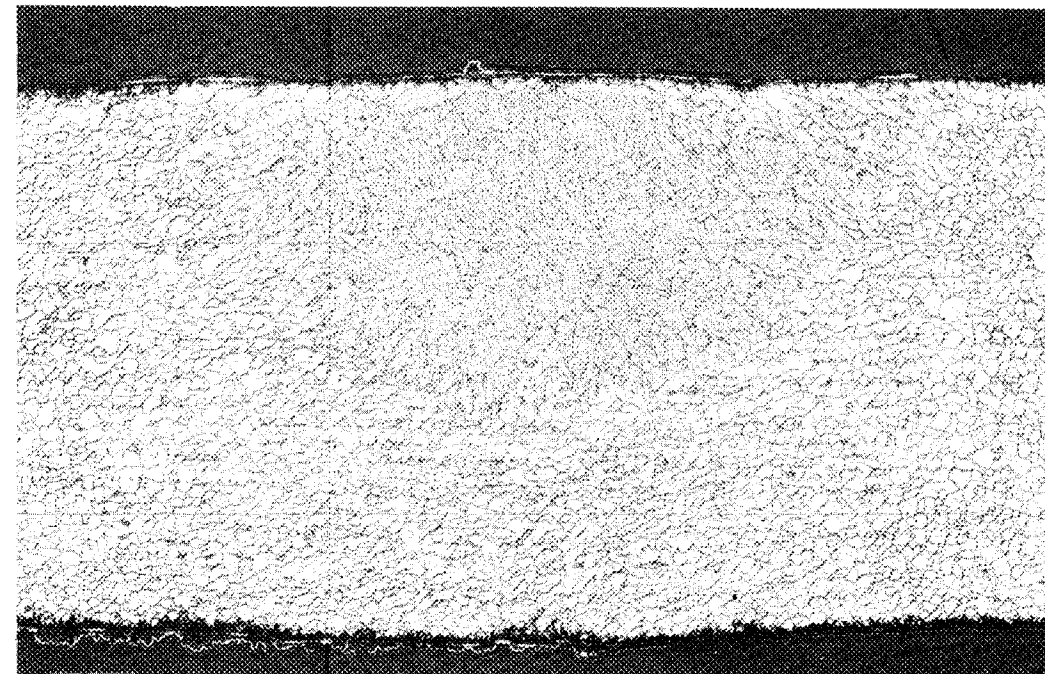
Y-188887



(a)

800 μm

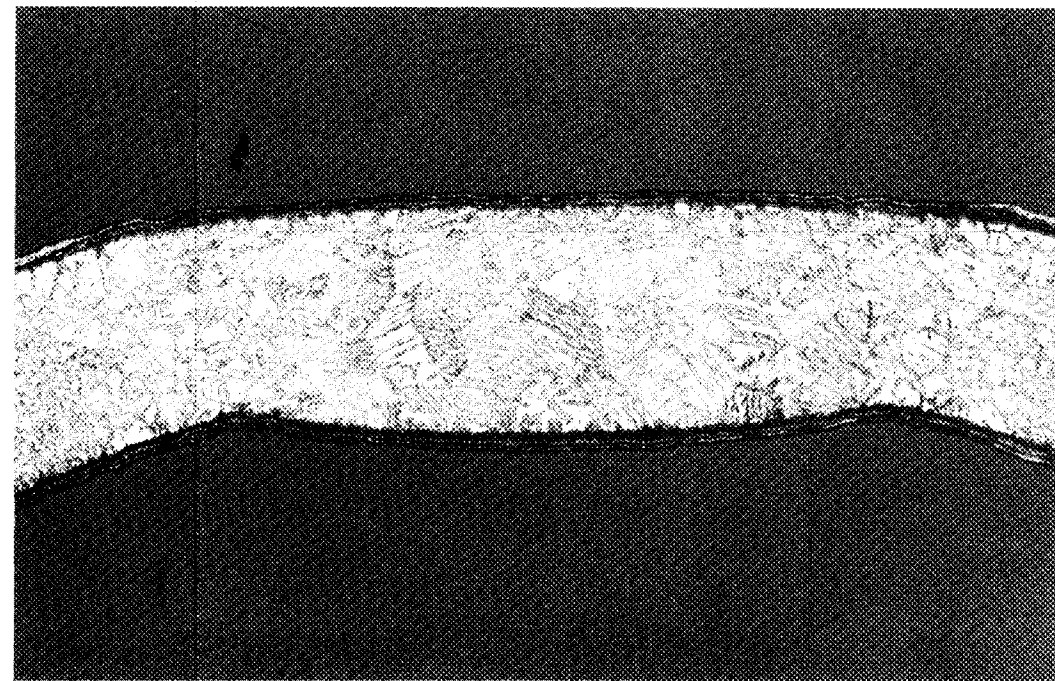
Y-188918



(b)

800 μm

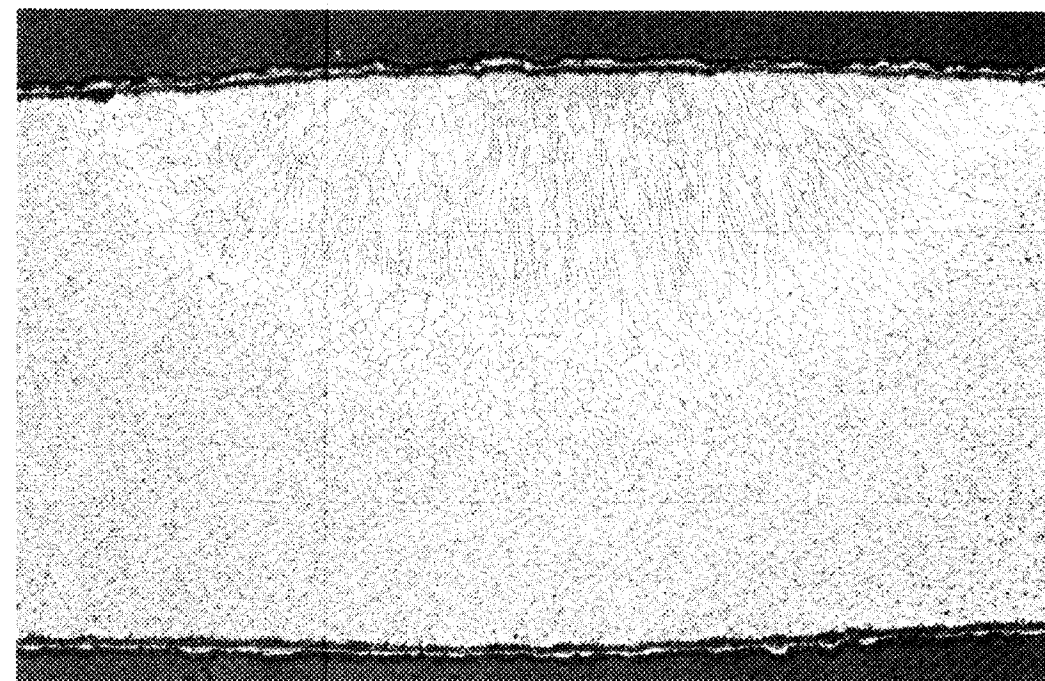
Y-188889



(c)

606 μm

Y-188919



(d)

800 μm

Fig. 10. Microstructures of welded specimens after exposure to synthetic flue gas. (a) Plain carbon steel. (b) Type 405 stainless steel. (c) Type 316 stainless steel. (d) Alloy 800. Etchant: aqua regia.

gases at about the same temperatures. Actual flue gases in the cases presented in Table 2 were incinerator combustion products containing elements and compounds derived from the waste materials being burned.⁶⁻⁹ Analysis of the corrosion products revealed the presence of some of the elements, and these might have aggravated corrosion. The corrosion rates obtained in the present study with synthetic flue gases were similar to those obtained in previous studies with synthetic flue gases. For example, the corrosion rate of steel in synthetic flue gases at about 550°C was 0.1 $\mu\text{m}/\text{h}$ after 256 h in a previous study¹⁰ and about 0.08 $\mu\text{m}/\text{h}$ after 500 h in the present study. The corrosion rate of type 321 stainless steel was 0.05 $\mu\text{m}/\text{h}$ after 450 h at 700°C in a previous study,¹⁰ while type 316 stainless steel corroded at the rate of about 0.08 $\mu\text{m}/\text{h}$ after 500 h at 660°C in the present study. Thus, the results obtained in this study for plain carbon steel and type 316 stainless steel agree with those of a previous study in which exposure times were a few hundred hours.

Plain carbon steel and type 405 stainless steel were tested at temperatures significantly above their anticipated use temperatures in the FBWHRS. The data indicate that plain carbon steel, if exposed continuously to flue gases at 560°C, would corrode at a rate exceeding 0.6 mm/year (0.02 in./year). The actual corrosion rate would depend on the frequency of scale removal due to thermal cycling or other reasons. Type 405 stainless steel, even at 560°C, still exhibited a projected corrosion rate of only 0.08 mm/year (0.003 in./year). Type 316 stainless steel and alloy 800, which were tested at temperatures approximately the same as their anticipated use temperatures in the FBWHRS, exhibited projected corrosion rates of 0.2 and 0.1 mm/year (0.008 and 0.004 in./year), respectively. These materials might also corrode at higher rates if the corrosion products were frequently removed by erosion or some other means to expose fresh surfaces.

Removal of corrosion products by erosion is likely to occur in the FBWHRS. Some areas of the distributor plate, containment walls, and steam generator tubes will be subjected to the scrubbing action of the bed medium. Metal wastage might therefore be accelerated by both erosion and

corrosion. This would be especially important when the inlet gas temperature is increased from 650 to 1000°C, as is being considered for an advanced version of the device. Future work should include combined erosion-corrosion studies at higher temperatures than those used in the present study.

The possibilities of intergranular corrosion and stress corrosion cracking should also be considered in future work. The present work showed that carbides precipitated at grain boundaries of type 316 stainless steel and alloy 800 during the corrosion test at temperatures of interest to the FBWHRs. Because the carbides typically contain chromium, migration of chromium to grain boundary precipitates results in lower chromium content in regions adjacent to grain boundaries. These regions are susceptible to intergranular attack in corrosive environments, such as condensate occurring during periods when the FBWHR is shut down. Another phenomenon, stress corrosion cracking, does not require grain boundary precipitation. Instead, stainless steels and other materials fail in certain environments, especially those containing aqueous chlorides, by crack propagation at stresses well below yield stresses. Because many aluminum remelt furnaces contain chlorides, stress corrosion might occur when aqueous condensate is present. The present work has not addressed either of these possible corrosion mechanisms.

The results that we have presented indicate that corrosion of candidate FBWHR materials in the aluminum remelt furnace atmosphere will not be significant at anticipated operating temperatures for various components. Factors that could cause higher corrosion rates include higher temperatures, frequent thermal cycles, erosion, and the presence of other elements and compounds in the flue gas. In particular, deposition of combustion products might aggravate corrosion, as is indicated in the results of previous studies involving actual flue gases.

ACKNOWLEDGMENTS

The author wishes to acknowledge the assistance of others in performing this work: P. J. Jones for specimen preparation, construction of

the gas metering systems, and conducting the test; W. H. Warwick and J. R. Mayotte for metallography and measurement of depth of corrosion; O. B. Cavin for x-ray diffraction; R. S. Crouse for electron microprobe analysis; Fay Burns for typing the draft; J. H. DeVan and M. J. Kania for technical review; Sigfred Peterson for technical editing; and D. L. LeComte for final typing and preparation of the report.

REFERENCES

1. *High Temperature Burner-Duct Recuperator System Progress Report for January 1983*, 81-18493(16), Garrett AiResearch Manufacturing Company, Torrance, Calif., Feb. 21, 1983.
2. M. Coombs, D. Kotchick, and H. Strumpf, *High Temperature Ceramic Recuperator and Combustion Air Burner Programs Semiannual Report for May 1982 through October 1982*, GRI-80/0165, Garrett AiResearch Manufacturing Company, Torrance, Calif., October 1982.
3. *High Temperature Fluid-Bed Heat Recovery for Aluminum Melting Furnace*, DOE/ID/12303-1, Aerojet Energy Conversion Company, Sacramento, Calif., December 1982.
4. G. Heinemann, F. G. Garrison, and P. A. Haber, "Corrosion of Steel by Gaseous Chlorine," *Ind. Eng. Chem.* **38**(5), 497-99 (May 1946).
5. M. H. Brown, W. B. DeLong, and J. R. Auld, "Corrosion by Chlorine and by Hydrogen Chloride at High Temperatures," *Ind. Eng. Chem.* **39**(7), 838-44 (July 1947).
6. P. D. Miller and H. H. Krause, "Factors Influencing the Corrosion of Boiler Steels in Municipal Incinerators," *Corrosion (Houston)* **27**(1), 31-45 (January 1971).
7. H. H. Krause, D. A. Vaughn, and P. D. Miller, "Corrosion and Deposits from Combustion of Solid Waste," *J. Eng. Power* **95**, 45-52 (January 1973).
8. H. H. Krause, D. A. Vaughn, and P. D. Miller, "Corrosion and Deposits from Combustion of Solid Waste, Part 2 - Chloride Effects on Boiler Tube and Scrubber Metals," *J. Eng. Power* **96**, 216-22 (July 1974).

9. D. A. Vaughn, H. H. Krause, and W. K. Boyd, "Fireside Corrosion in Municipal Incinerators Versus Refuse Composition," *Mater. Perform.* **14**(5), 16-24 (May 1975).

10. P. Mayer and A. V. Manolescu, "Influence of Hydrogen Chloride on Corrosion of Boiler Steels in Synthetic Flue Gas," *Corrosion (Houston)* **36**(7), 369-73 (July 1980).

INTERNAL DISTRIBUTION

- | | | | |
|--------|-------------------------------|-----|------------------------------|
| 1-2. | Central Research Library | 22. | L. E. McNeese |
| 3. | Document Reference Section | 23. | A. J. Moorhead |
| 4-5. | Laboratory Records Department | 24. | A. R. Olsen |
| 6. | Laboratory Records, ORNL RC | 25. | A. C. Schaffhauser |
| 7. | ORNL Patent Section | 26. | G. M. Slaughter |
| 8. | R. A. Bradley | 27. | J. O. Stiegler |
| 9. | R. S. Carlsmith | 28. | R. J. Charles (Consultant) |
| 10. | P. T. Carlson | 29. | Alan Lawley (Consultant) |
| 11-13. | F. R. Cox | 30. | T. B. Massalski (Consultant) |
| 14-18. | J. I. Federer | 31. | R. H. Redwine (Consultant) |
| 19. | J. P. Hammond | 32. | J. C. Williams (Consultant) |
| 20. | R. R. Judkins | 33. | K. M. Zwilsky (Consultant) |
| 21. | W. J. Lackey | | |

EXTERNAL DISTRIBUTION

- 34-36. Aerojet Energy Conversion Company, P.O. Box 13222,
Sacramento, CA 95813
- Kenneth L. Gustafson
Kenneth E. Unmack
Howard Williams
- 37-38. Airesearch Manufacturing Co. of California, 2525 W. 190th St.,
Torrance, CA 90509
- M. Coombs
D. Kotchick
39. Babcock and Wilcox Company, Lynchburg Research Center,
Lynchburg, VA 24505
- J. E. Snyder
- 40-41. EG&G Idaho, Inc., P.O. Box 1625, Idaho Falls, ID 83415
- Scott Richlen
Dan Suciu

42. Electric Power Research Institute, 3412 Hillview Ave.,
P.O. Box 10412, Palo Alto, CA 94303
- 43-44. Gas Research Institute, 8600 W. Bryn Mawr, Chicago, IL 60631
C. J. Dobos
W. W. Liang
- 45-46. Solar Turbines, Inc., P.O. Box 80966, San Diego, CA 92138
A. D. Russell
M. E. Ward
47. Thermo Electron Corporation, P.O. Box 459, Waltham, MA 02254
Robert DeSaro
- 48-49. DOE, IDAHO OPERATIONS OFFICE, 550 Second Street, Idaho, ID 83401
John B. Patton
W. H. Thielbahr
- 50-52. DOE, INDUSTRIAL PROGRAMS, Office of Assistant Secretary,
Conservation and Solar Energy, Forrestal Bldg.,
1000 Independence Ave., Room 2H085, Washington, DC 20585
J. N. Eustis
A. Hayes
J. W. Osborne
53. DOE, WASTE HEAT RECOVERY BRANCH, MS 5F--035, Forrestal Building,
1000 Independence Avenue, Washington, DC 20585
Program Manager
54. DOE, OAK RIDGE OPERATIONS, OFFICE, P.O. Box E, Oak Ridge, TN 37830
Office of Assistant Manager for Energy Research and Development
- 55-181. DOE, TECHNICAL INFORMATION CENTER, Office of Information Services,
P.O. Box 62, Oak Ridge, TN 37830